A novel activated carbon prepared from grapefruit peel and its application in removal of phenolic compounds

Xiao Liu, Yibei Wan, Penglei Liu, Yanzhen Fu and Weihua Zou

ABSTRACT

The most ideal conditions for preparing activated carbon from grapefruit peel (GPAC) were studied using $NH_4H_2PO_4$ as a chemical activating agent and the obtained material was characterized by scanning electron microscopy (SEM), Fourier transform infrared spectroscopy (FTIR) and Brunauer–Emmett–Teller (BET) analysis. The adsorption capacity of the resulting material has been checked using three phenolic compounds (pyrocatechol (CA), 4-chlorophenol (4-CP) and 2,4-dichlorophenol (2,4-DCP)). The adsorption characteristics of phenolic compounds from aqueous solution by GPAC have been investigated as a function of contact time, pH, initial concentration and temperature. The equilibrium experimental data fitted well with Freundlich and Koble–Corrigan isotherms. The adsorption of the three phenolic compounds on GPAC fitted well with pseudo-second-order kinetic model. Different thermodynamic parameters were also evaluated and it was found that the adsorption was spontaneous, feasible and endothermic in nature. Adsorbents were regenerated by 0.1 mol/L NaOH and GPAC could be reused in phenolic compounds removal.

Key words | adsorption, grapefruit peel-based activated carbon (GPAC), $NH_4H_2PO_4$, phenolic compounds

Xiao Liu
Yibei Wan
Penglei Liu
Yanzhen Fu
Weihua Zou (corresponding author)
School of Chemical Engineering and Energy,
Zhengzhou University,
100# of Kexue Road, Zhengzhou 450001,
China
E-mail: *whzou@zzu.edu.cn*

INTRODUCTION

Phenolic compounds, including a wide variety of organic chemicals, are the most common water pollutants. The major sources of phenol pollution are waste waters from paint, pesticide, coal conversion, polymeric resin, dyes, explosives, insecticides, petroleum and petrochemicals industries (Dabrowski *et al.* 2005). Phenol can be generated by human activities and nature. Phenolic waste disposal into water not only affects human beings but also influences flora and fauna. Thus it is important to remove it for the sake of our health (Ahmaruzzaman 2008).

Many conventional methods used to remove phenolic compounds from aqueous solutions include ion-exchange, solvent extraction, coagulation, chemical precipitation, adsorption and reverse osmosis (Dursun *et al.* 2005). Adsorption is an effective method for the elimination of phenolic compounds from water and some commonly used adsorbents (Ahmaruzzaman & Sharma 2005) include natural minerals (Yousef *et al.* 2011; Dudziak & Werle 2016), resins (Li *et al.* 2001; Lin & Rueyshin 2009), activated carbon (Loredocancino *et al.* 2016) and so on. In recent years, many researchers have tried to produce low-cost activated carbons for removal of the pollutants using renewable and cheaper material which were mainly industrial and agricultural by-products (Mallampati *et al.* 2015). Singh *et al.* prepared the activated carbon from waste Parthenium to remove *p*-cresol from aqueous solution (Singh *et al.* 2008). Loredocancino *et al.* researched the adsorption and desorption of phenol using the barley husk-activated carbon (Loredocancino *et al.* 2016). Prashanthakumar *et al.* investigated the removal of toxic phenolic compounds using porous carbon prepared from renewable biomass coconut spathe (Prashanthakumar *et al.* 2018).

Grapefruit is the third most important citrus crop in the world, with approximately 4 million metric tons of world yearly output. A whole grapefruit comprises 44–54% peel. Production of grapefruit is high and large quantities of grapefruit peel is thrown away after consumption, resulting in waste of resources and an environmental problem (Chai *et al.* 2015). Grapefruit peel contains several water soluble and insoluble monomers and polymers. These polymers are rich in carboxyl and hydroxyl functional groups, thus making it a potential adsorbent material for the removal of heavy metals or dyes from aqueous solutions (Torab-Mostaedi *et al.* 2013;

doi: 10.2166/wst.2018.212

Zou *et al.* 2013b, 2013c; Zhang *et al.* 2015). To make use of this abundant waste as an adsorbent, it is proposed to transform it into activated carbon (Pei & Liu 2012; Huang *et al.* 2014).

Activated carbons are generally prepared from agricultural by-products by physical or chemical activations. Recent works have demonstrated the possibility of developing activated carbon from grapefruit peel by chemical activation with NaOH or $ZnCl_2$ for the removal of dyes from aqueous solution (Pei & Liu 2012; Huang *et al.* 2014; Nowicki *et al.* 2016). However, using NaOH as the activating agent could corrode the instruments and $ZnCl_2$ has harmful effects on the environment. Therefore, alternative chemicals which can be used as activating agents have received increasing attention in recent years. There is little information about the feasibility of preparing activated carbon with ammonium phosphates activation, such as $NH_4H_2PO_4$. The $NH_4H_2PO_4$ is alkaline at low temperature and it can decompose into ammonia and pyrophosphate at 403 K. When the temperature is above 673 K, condensed phosphates are formed. At higher temperature, the reaction between the grapefruit peel and $NH_4H_2PO_4$ becomes more intense, which promotes the decomposition of grapefruit peel and develops the porous structure. In addition, the generated gas (NH_3) may have a significant effect on the formation of pores during the pyrolysis of grapefruit peel. For this reason, the main goal of this study was to prepare the low-cost carbonaceous adsorbents from grapefruit peel with $NH_4H_2PO_4$ activation.

The optimum activation conditions (such as impregnation times, activation temperatures and activator concentration) of grapefruit peel with $NH_4H_2PO_4$ were investigated to enhance the adsorption capacity for phenolic compounds (CA, 4-CP and 2,4-DCP) from aqueous solution. Influencing factors on grapefruit peel-based activated carbon (GPAC) adsorption, including contact time, temperature, pH, initial concentrations and surface property of the GPAC, were investigated. The adsorption mechanism of GPAC was discussed according to the kinetic experimental results.

MATERIALS AND METHODS

Adsorbates

All chemicals and reagents used in the study were of analytical grade. The stock solutions of 1,000 mg/L phenolic compounds were prepared by dissolving 1 g of each adsorbate in a 1 L volumetric flask and then diluting appropriately with distilled water to prepare the working solutions. The initial pH of the working solution was adjusted by addition of HCl and NaOH solution.

Adsorbents preparation

Grapefruit peel was crushed to a size of 0.5 cm, washed with distilled water and dried. The dried grapefruit peel was impregnated in $NH_4H_2PO_4$ solution in a weight ratio of 1:10 for 2 h, 5 h, 10 h and 15 h at room temperature. The mass percentage concentration of $NH_4H_2PO_4$ was 5%, 10%, 20% and 30%, respectively. The immersed samples were then dried at 373 K for 8 h. The pretreated precursors were heated up to 573–1,073 K for 1 h in a tubular furnace under the protection of nitrogen to obtain carbonized materials. The activation products were washed thoroughly with deionized water until the activated carbon became neutral. The samples were dried at 348 K for 2 h and sieved into uniform granules of 0.9–0.42 mm for further use.

Characterization of GPAC

The Fourier transform infrared spectroscopy (FTIR) was recorded on a PE-1710 FTIR spectrometer in the range of 400–4,000 cm^{-1} with KBr pellets. The surface morphology of grapefruit peel and GPAC were observed by scanning electron microscopy (SEM) (JEOL JSM-7500F). The specific surface area and pore structural parameters of GPAC were assessed by nitrogen adsorption–desorption analysis (NOVA4200e, Quantachrome). Zero point of charge (pH_{pzc}) of GPAC was determined using the method described by Moreno-Castilla *et al.* (Moreno-Castilla *et al.* 2000).

Adsorption experiments

The effect of initial pH on the removal of phenolic compounds was analyzed in the pH range of 2–12. The initial concentration of the three phenolic compounds was 4 mmol/L. Equilibrium and kinetic experiments were carried out at initial pH 5.0. The equilibrium studies were performed by adding 0.01 g of GPAC and 10 mL of CA, 4-CP or 2,4-DCP solutions (2–8 mmol/L) to the Erlenmeyer flasks. The flasks were agitated in a mechanical shaker (120 rpm) until equilibrium was reached. Kinetic studies were performed by adding 0.01 g of GPAC into flasks containing 10 mL of CA, 4-CP or 2,4-DCP solutions of known initial concentration. Distilled water was used as a blank solution. Residual concentration of CA, 4-CP and 2,4-DCP solutions were measured by visible spectrophotometry

using a UV spectrophotometer (Shimadzu UV-3000) at λ_{max} of 275, 279 and 286 nm, respectively. All the adsorption experiments were performed in duplicate. The adsorption capacity of GPAC for phenolic compounds was calculated using the following equations:

$$q_t = \frac{(C_i - C_t)V}{m} \quad (1)$$

$$q_e = \frac{(C_i - C_e)V}{m} \quad (2)$$

where q_t and q_e are the adsorption capacity of phenolic compounds at time t and equilibrium (mmol/g), respectively. C_i is the initial concentration of solutions for phenolic compounds (mmol/L). C_t and C_e are the liquid-phase concentrations of phenolic compounds at time t and equilibrium (mmol/L), respectively. V is the volume of solutions for phenolic compounds (L) and m is the weight of GPAC (g).

Desorption tests

In order to determine the reusability of GPAC, consecutive adsorption–desorption cycles were repeated three times. In this study, 0.1 mol/L NaOH solution was used as the desorbing agent. The GPAC loaded with CA, 4-CP or 2,4-DCP was placed in the conical flasks and was constantly stirred on a rotatory shaker (100 rpm) for 480 min at 298 K. After each cycle of adsorption and desorption, the adsorbent was washed with distilled water and reconditioned for adsorption in the succeeding cycle.

RESULTS AND DISCUSSION

Optimum conditions for the prepared GPAC used for the adsorption of phenolic compounds

Effect of impregnated time on GPAC properties

The effect of impregnated time on the adsorption of phenolic compounds by GPAC was studied at room temperature. The initial concentration of CA, 4-CP or 2,4-DCP was 2 mmol/L. With the increase in impregnated time from 2 h to 15 h, the adsorption capacities of GPAC for CA, 4-CP and 2,4-DCP increased from 0.30, 0.40 and 0.81 mmol/g to 0.40, 0.60 and 1.15 mmol/g, respectively. When the impregnated time was 5 h, the adsorption capacities of GPAC for CA, 4-CP and 2,4-DCP reached 0.396, 0.598 and 1.148 mmol/g, respectively. It was observed that adsorption capacities were not obvious when impregnated time was more than 5 h. In other words, activated carbon with higher adsorption capacity was obtained at impregnated time of 5 h.

Effect of activation temperature

The activation of an impregnated material further accelerates thermal degradation and the volatilization process. This leads to the development of pores and an increase in surface area. Activation temperature affects both the BET surface area and the development of micropore/mesopore. It showed that the adsorption capacity of CA, 4-CP or 2,4-DCP increased with increasing activation temperature from 573 to 873 K. This phenomenon suggested that the light constituents or volatile compounds in grapefruit peel were released with the increase of activation temperature leading to the development of more pores and adsorption sites. Another reason may be related to the pyrolysis of grapefruit peel-$NH_4H_2PO_4$. The generated gas (NH_3) may have a significant effect on the formation of pores, especially for micropores. However, the adsorption capacity of GPAC was decreased with the activation temperature increasing from 873 K to 1,073 K. It may induce shrinkage in the structure of GPAC, resulting in the reduction of surface area and total pore volume.

Effect of $NH_4H_2PO_4$ concentration on GPAC properties

The important factor for the development of porosity in activated carbon is the activator concentration. This study showed that the adsorption capacity of phenolic compounds on GPAC increased as the activator concentration increased from 5% to 30%. The higher concentration of $NH_4H_2PO_4$ can produce larger quantities of NH_3 and H_3PO_4, which increased specific surface area and the sites of adsorption. However, the increase of the adsorption capacity is not significant when the $NH_4H_2PO_4$ concentration was between 20% and 30%, which indicated that there no more pores were formatted by the extra $NH_4H_2PO_4$.

Characterization of GPAC

FTIR analysis

The FTIR spectra of GPAC and GPAC-adsorbed CA, 4-CP or 2,4-DCP is shown in Figure 1. The broad absorption band at around 3,400–2,400 cm^{-1} could be assigned to the

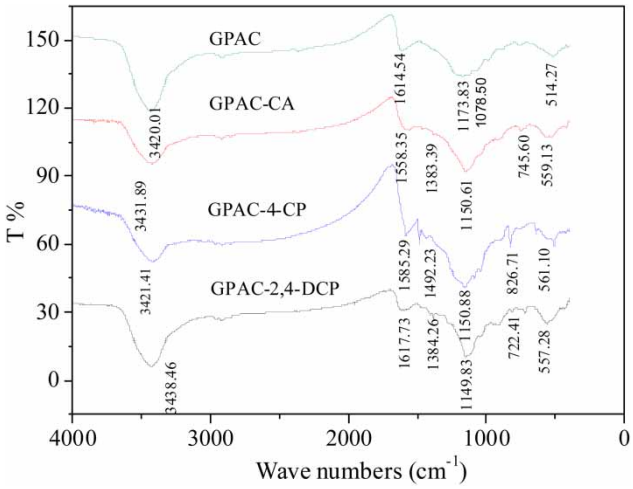

Figure 1 | FTIR spectra of GPAC and GPAC-adsorbed CA, 4-CP and 2,4-DCP.

stretching vibration of hydroxyl functional groups. The band at 1,631–1,561 cm^{-1} is ascribed to the vibrations of aromatic C = C for activated carbons obtained from $NH_4H_2PO_4$ activation. The band at 1,228–1,131 cm^{-1} was assigned to stretching vibration of carbonic group ν(–CO). These bands are commonly found in four activated carbons. The strong peak located at 1,082–1,059 cm^{-1} may be ascribed to the stretching mode of hydrogen-bonded P = O, O–C stretching vibrations in the P–O–C linkage, and P = OOH. It indicates that phosphoric acid produced by thermal decomposition of $NH_4H_2PO_4$ is successfully infiltrated into GPAC. Therefore, P-containing carbonaceous structures like acid phosphates and polyphosphates are formed in the GPAC (Shaarani & Hameed 2011; Yorgun Yıldız 2015). The peak at 590, 519, 514 and 581 cm^{-1} were caused by plane external bending of C–H for different substituted benzene rings (Kong *et al.* 2013). The result of FTIR spectroscopy indicates that the produced carbons are rich in surface functional groups.

From Figure 1, it can be observed that the frequency of absorption peaks on the surface of GPAC had changed slightly after adsorbing CA, 4-CP or 2,4-DCP, which suggested that there was a binding process taking place. The band at 1,614.54 cm^{-1} was shifted to 1,558.35, 1,585.29 and 1,617.73 cm^{-1} when the GPAC adsorbed CA, 4-CP or 2,4-DCP, respectively. It is mainly attributed to the dispersive interactions between the π-electrons of the benzene rings in phenolic compounds and the electron-rich region in the aromatic ring of the substrate. For the adsorption of CA on GPAC, new peaks at 1,383.99 and 745.60 cm^{-1} were observed. The same changes were also observed in the spectra after 4-CP (or 2,4-DCP) adsorption onto GPAC. New peaks at 1,492.23 and 826.71 cm^{-1} (or 1,384.26 and 722.41 cm^{-1}) were observed. The peaks at 1,383.99 cm^{-1} (CA) or 1,384.26 cm^{-1} (2,4-DCP) were due to O–H bending of CA or 2,4-DCP. The peak at 1,492.23 cm^{-1} is attributed to the aromatic ring-breathing modes of adsorbed 4-CP. Therefore, three phenolic compounds were adsorbed on the surface of GPAC (Kyzas & Deliyanni 2014).

SEM of GPAC

The SEM micrographs of grapefruit peel and GPAC are presented in Figure 2. The texture of the grapefruit peel was fairly coarse with less cracks and voids, and the activated carbon surface was composed of pores with a tunnel shape and overall honeycomb structure. In the process of chemical activation, the raw grapefruit peel was impregnated by $NH_4H_2PO_4$. The impregnated grapefruit peel is

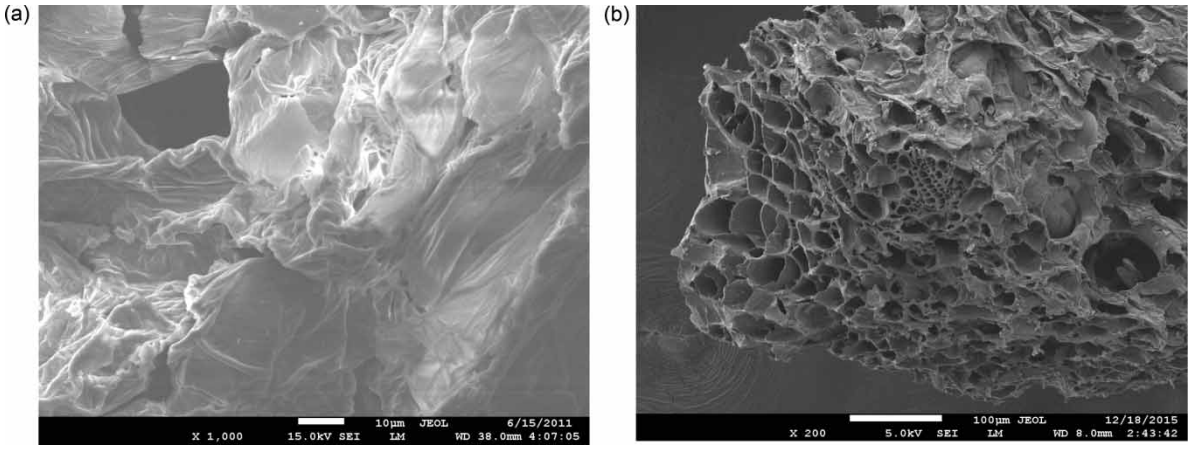

Figure 2 | SEM image of (a) grapefruit peel and (b) GPAC.

pyrolytic. The dehydration of the cellulosic material resulted in charring and aromatization of the carbon skeleton during pyrolysis, which developed the porous structure. Upon $NH_4H_2PO_4$ activation, more porous structures began to appear, which can be attributed to the decomposition of $NH_4H_2PO_4$ into ammonia and phosphoric acid. H_3PO_4 acted as a catalyst for the catalytic cracking of large molecules in organic compounds during the carbonization step. The phenomenon indicated that there was a good pore formation in the preparation of activated carbons using $NH_4H_2PO_4$ as an activator.

Specific surface area and pore structural characterization analysis of the GPAC

The N_2 adsorption–desorption isotherms and pore size distributions were used to confirm the textural properties of GPAC. It displayed type IV isotherms with clear hysteresis loops at virtual P/P_0 in between 0.32 and 0.95 associated with capillary condensation. The data of the total surface area calculated from the isotherm were 221.817 m^2/g and the average pore radius of the GPAC was found as 3.71 nm. Sun *et al.* produced activated carbon from *Cyperus alternifolius* using $H_4P_2O_7$ activation and the S_{BET} was 1,066 m^2/g (Sun *et al.* 2012). Marzbali *et al.* produced activated carbon from apricot nut shells using H_3PO_4 activation and the S_{BET} was 307.6 m^2/g (Marzbali *et al.* 2016). Thuan *et al.* prepared activated carbon from banana peel using KOH activation and the S_{BET} was 63.5 m^2/g (Thuan *et al.* 2017). The porous structures increased the specific surface area of GPAC. The pore size distributions of GPAC show that a vast majority of the pores fall into the range of mesopore (3–50 nm).

Adsorption studies

The adsorption capacity of GPAC for phenolic compounds depends on the nature of both the adsorbent (such as pore structure, functional groups) and adsorbate (such as its pK_a, functional groups, polarity, molecular weight and size). The adsorption capacity of GPAC depends also on the solution conditions such as pH, the adsorbate concentration, ionic strength and temperature.

Effect of pH

The pH_{pzc} of an adsorbent is a very important characteristic. The pH_{pzc} of GPAC was evaluated to be 4.10, indicating the surface is positively charged at $pH < 4.10$ and negatively charged at $pH > 4.10$.

The initial pH value of a solution is one of the most important factors influencing phenolic compound adsorption. Figure 3 shows the different pH behavior of the GPAC for CA, 4-CP and 2,4-DCP removal. It can be seen that the pH value of solution has small influence on the adsorption capacity in the pH range of 2–7. However, with increasing pH value from 7 to 11, the value of q_e obviously decreased. For example, the adsorption uptake of 2,4-DCP onto GPAC increased slightly with the solution pH increasing from 2 to 5 and then decreased sharply with the increase of pH from 5 to 11. The pK_a value for 2,4-DCP is 7.7, indicating adsorbing species were mostly non-ionized. The electrostatic attraction improved with the decreasing number of H^+ when the solution pH was between 2 and 5. With the increase of pH from 5 to 11, electrostatic repulsion between the surface of GPAC and the anionic phenolate results in the decreasing of adsorption capacity. In addition, phenolate anions with greater solubility can form a stronger bond with water molecules, which decreased the hydrophobicity of chlorophenols. Thus, the adsorption capacity of phenolic compounds on GPAC decreased sharply under alkaline conditions (Başar 2006). The maximum adsorption capacity for CA onto GPAC was obtained at pH 9. The adsorption capacities increased slightly with the pH increasing from 2 to 9 and then slightly decreased with the pH increasing from 9 to 11. The result suggested that a hydrogen bond may exist between the CA and hydroxy or amino group contained in GPAC.

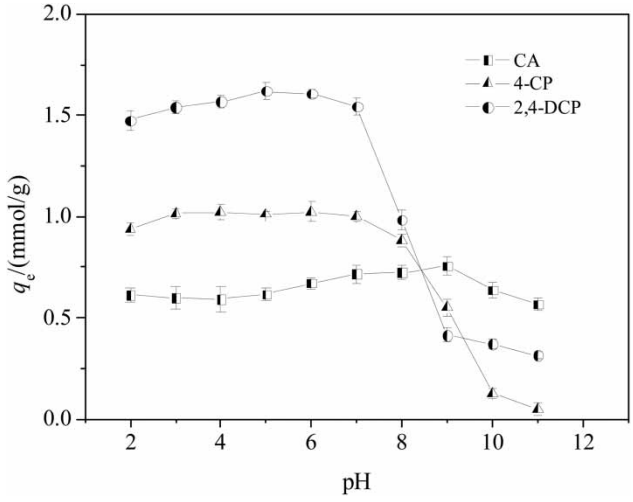

Figure 3 | Effect of initial pH on the removal of phenolic compounds by GPAC.

Adsorption kinetic

The controlling mechanism of the adsorption process was investigated by fitting the experimental data with the pseudo-first-order kinetic model (Equation (3)), pseudo-second-order kinetic model (Equation (4)) and intraparticle diffusion model (Equation (5)).

$$q_t = q_e(1 - e^{-k_1 t}) \tag{3}$$

$$q_t = \frac{k_2 q_e^2 t}{1 + k_2 q_e t} \tag{4}$$

$$q_t = k_{id} t^{1/2} + C \tag{5}$$

where q_e and q_t are the adsorption capacity at equilibrium and at any time t, respectively (mmol/g); k_1 and k_2 is the rate constant of pseudo-first-order model (min^{-1}) and pseudo-second-order model (g/mmol·min), respectively. k_{id} is the intraparticle diffusion rate constant (g/mmol·$min^{1/2}$) and C is a constant that provides information regarding the thickness of the boundary layer.

The relative parameters are listed in Table 1 and the fitted curves are depicted in Figure 4. It can be seen from Table 1 that the higher values of R^2 and lower values of SSE showed that the pseudo-second-order model was better for predicting the kinetic process. The results indicated that the adsorption process of CA, 4-CP and 2,4-DCP onto GPAC included chemisorption. Figure 4(a) typically illustrates the comparison between the calculated and measured results for the adsorption of phenolic compounds on GPAC. The calculated values of equilibrium adsorption capacity obtained from the pseudo-second-order model for CA, 4-CP and 2,4-DCP were 0.651, 1.060 and 1.639 mmol/g, respectively. The removal efficiency is in the order of 2,4-DCP > 4-CP > CA. It is known that the adsorption capacity of GPAC depends on the solubility of the phenolic compounds and the hydrophobicity of the substituent.

Weber and Morris showed the fractional uptake of the adsorbate was a function of square root of time $t^{1/2}$ rather than time t (Weber & Morris 1963; Kumar 2007). On this basis, the intraparticle diffusion model (Figure 4(b)) was used to investigate the mechanisms and rate-controlling steps affecting the kinetics of adsorption (Başar 2006). The low values of SD indicated the linear model was well fitted. The intraparticle diffusion model showed the characteristics of multi-linearity, indicating that two steps take place during the adsorption process. The first portion of the plots, attributed to the diffusion of phenolic compounds from the solution to the exterior surface of GPAC, was fastest. After the exterior surface reached saturation, the molecules of phenolic compounds entered into the pores of GPAC and were adsorbed by the interior surface of the adsorbents. It can be seen that the plot did not pass through the origin, indicating the intraparticle diffusion was not the only rate-controlling step. The C value represented the thickness of boundary layer and can be determined from the intercept of the linear plots. Table 1 indicates that the order of adsorption rate is k_{id1}(2,4-DCP) > k_{id1}(4-CP) > k_{id1}(CA). Meanwhile, the same order was observed for the values of k_{id2}. This suggests that the solubility and the hydrophobicity affects the diffusion rate of phenolic compounds from solution to the hydrophobic surfaces of GPAC.

Table 1 | Kinetic parameters of phenolic compounds adsorption onto GPAC

Parameters	CA	4-CP	2,4-DCP
Pseudo-first-order			
k_1 (min^{-1})	0.161	0.104	0.034
$q_{e,cal}$ (mmol/g)	0.629	1.008	1.520
$q_{e,exp}$ (mmol/g)	0.664	1.093	1.610
R^2	0.9156	0.9062	0.8948
$SSE \times 10$	0.065	0.350	2.501
Pseudo-second-order			
k_2 (g/mg·min)	0.413	0.142	0.032
$q_{e,cal}$ (mmol/g)	0.651	1.060	1.639
R^2	0.9882	0.9827	0.9627
$SSE \times 10$	0.029	0.065	0.597
Intraparticle diffusion			
k_{id1} (mmol/g·$min^{1/2}$) $\times 10$	0.393	0.563	1.041
C_1	0.325	0.443	0.300
R_1	0.9275	0.9185	0.9880
$SD \times 10$	0.479	0.990	0.665
k_{id2} (mmol/g·$min^{1/2}$) $\times 10^2$	0.399	0.918	2.056
C_2	0.575	0.880	1.182
R_2	0.9843	0.9143	0.9750
$SD \times 10^2$	0.409	1.947	2.240

$$SSE = \sum_{i=1}^{n} (q_{cal} - q_{exp})_i^2$$

$$SD = \sqrt{\frac{\sum [(q_{exp} - q_{cal})/q_{exp}]^2}{n-1}}$$

Adsorption equilibrium

The effect of the equilibrium concentration of CA, 4-CP and 2,4-DCP on the values of q_e is shown in Figure 5. The values

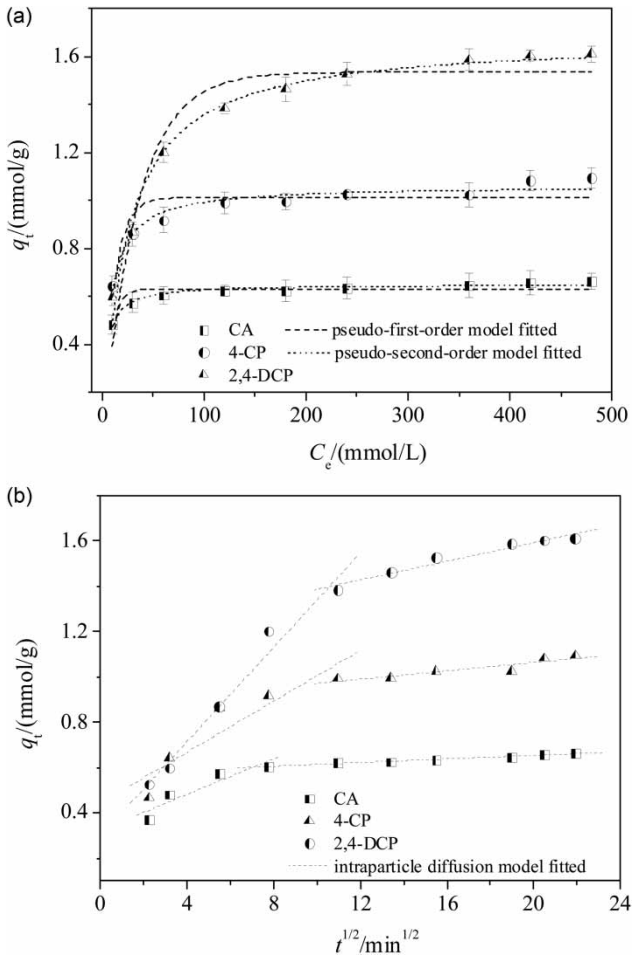

Figure 4 | Pseudo-first-order and pseudo-second-order (a) and intraparticle diffusion (b) models for the adsorption of phenolic compounds on GPAC ($C_{0\ (CA,\ 4\text{-}CP,\ 2,4\text{-}DCP)} = 4$ mmol/L).

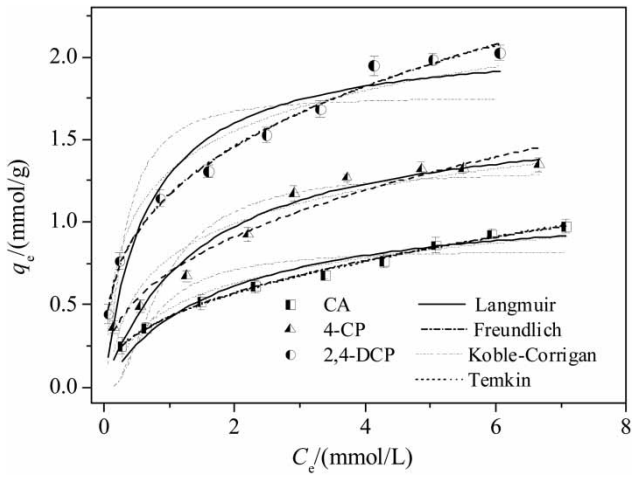

Figure 5 | Adsorption isotherms for the adsorption of CA, 4-CP and 2,4-DCP on GPAC at 298 K.

of q_e increased with increasing phenolic compounds concentration. The phenolic compounds concentration provided the necessary driving force to overcome the resistances to the mass transfer of adsorbents between the aqueous and solid phases. The increase in phenolic compounds concentration also enhanced the interaction between adsorbates and GPAC. Therefore, an increase in adsorbates concentration enhanced the adsorption uptake of phenolic compounds. It can be also found that the adsorption capacities of three phenolic compounds on GPAC increased with the increasing number of Cl atoms. The −OH in phenolic compounds can form hydrogen bonds with −OH, $-NH_2$ and −COOH in GPAC. For the three phenolic compounds, the adsorption capacity of CA is the minimum, which is due to the formation of intramolecular hydrogen bonds. C–Cl of chlorophenol bond length is shorter, which leads to low solubility in water and is easily adsorbed by GPAC.

Equilibrium data is significant for the design of an adsorption system. In this work, the Langmuir isotherm model (Equation (6)), Freundlich model (Equation (7)), Koble–Corrigan model (Equation (8)) and Temkin isotherm model (Equation (9)) were applied to describe the adsorption equilibrium.

$$q_e = \frac{q_m K_L C_e}{1 + K_L C_e} \tag{6}$$

$$q_e = K_F C^{1/n} \tag{7}$$

$$q_e = \frac{A C_e^n}{1 + B C_e^n} \tag{8}$$

$$q_e = A_T + B_T \ln C_e \tag{9}$$

where q_m and q_e is the maximum adsorption capacity and equilibrium absorption capacity (mmol/g), respectively; K_L is a Langmuir constant related to the affinity of the binding sites and energy of adsorption (L/mmol); K_F and $1/n$ are the Freundlich constants related to the adsorption capacity and adsorption intensity of the adsorbent, respectively. The Koble–Corrigan model is a three-parameters equation for equilibrium adsorption data. It is a combination of the Langmuir and Freundlich isotherm models. Values of A_T and B_T are the constant of Temkin isotherm model.

The parameters of the four models calculated on the basis of Equations (6)–(9) are listed in Table 2. The fitted curves at 298 K are also shown in Figure 5. From Table 2,

Table 2 | Isotherm constants for phenolic compounds adsorption by GPAC

	CA			4-CP			2,4-DCP		
Parameters	**298 K**	**308 K**	**318 K**	**298 K**	**308 K**	**318 K**	**298 K**	**308 K**	**318 K**
Langmuir									
q_{max} (mmol/g)	1.144	1.180	1.265	1.677	1.728	1.741	2.117	2.183	2.193
K_L (L/mmol)	0.574	0.649	0.802	0.689	0.718	0.839	1.547	1.983	2.984
R^2	0.9410	0.9598	0.9541	0.9352	0.9541	0.9353	0.9021	0.9539	0.9462
SSE	0.0262	0.0208	0.0287	0.0683	0.0556	0.0815	0.2198	0.1328	0.1617
Freundlich									
$1/n$	0.423	0.397	0.371	0.389	0.388	0.364	0.322	0.315	0.272
K_F(mmol/g(L/mmol)$^{1/n}$	0.426	0.473	0.558	0.695	0.725	0.788	1.165	1.261	1.414
R^2	0.9945	0.9981	0.9986	0.9504	0.9617	0.9680	0.9896	0.9745	0.9871
SSE	0.0024	0.0010	0.0010	0.0523	0.0464	0.0398	0.0229	0.0734	0.0387
Koble–Corrigan									
A	0.375	0.505	0.610	0.926	1.011	1.000	1.209	2.160	2.501
B	−0.119	0.068	0.091	0.325	0.387	0.262	0.035	0.633	0.689
n	0.354	0.437	0.418	0.590	0.637	0.502	0.335	0.545	0.465
R^2	0.9945	0.9983	0.9989	0.9505	0.9708	0.9713	0.9879	0.9850	0.9970
SSE	0.0021	0.0010	0.0010	0.0452	0.0353	0.0357	0.9011	0.0431	0.0092
Temkin									
A	0.474	0.517	0.609	0.780	0.788	0.864	1.306	1.381	1.541
B	0.223	0.231	0.243	0.303	0.338	0.324	0.355	0.408	0.358
R^2	0.9563	0.9690	0.9726	0.9239	0.9496	0.9419	0.9585	0.9873	0.9908
SSE	0.0221	0.0161	0.0172	0.0917	0.0610	0.0723	0.1046	0.0366	0.0277

$SSE = \sum_{i=1}^{n} (q_{e,cal} - q_{e,exp})_i^2$

it can be seen that the regression coefficient obtained from the Freundlich, Koble–Corrigan and Temkin isotherms are higher than those obtained from the Langmuir isotherm. Furthermore, the values of *SSE* were lower, which suggests that the Freundlich, Koble–Corrigan and Temkin models provided the better fit for the adsorption of phenolic compounds on GPAC than Langmuir model. The higher R^2 of the Koble–Corrigan model indicated a combination between heterogeneous and homogeneous adsorption of phenolic compounds. The values of $1/n$ in the Freundlich model between 0 and 1 are beneficial for adsorption phenolic compounds (Chowdhury *et al.* 2011). This result shows the multilayer coverage of adsorbate molecules on the surface of GPAC facilitated by heterogeneous sites present at the surface of sorbent (Gautam *et al.* 2015). The value of q_m obtained from the Langmuir isotherm of CA, 4-CP and 2,4-DCP is 1.144, 1.677 and 2.117 mmol/g at 298 K, respectively. From Table 2, it can be seen that the maximum adsorption capacity of GPAC (q_m) increased with the increasing of temperature from 298 K to 318 K. This result indicated that GPAC had a relatively stronger affinity for 2,4-DCP than CA and 4-CP, and the order of affinity was as follows: 2,4-DCP > 4-CP > CA. This result is also consistent with the foregoing conclusion derived from the kinetic model. In water, 4-CP strongly interacts with water by hydrogen bonding and is not significantly attracted to the hydrophobic surfaces of GPAC. Compared with 4-CP, 2,4-DCP interacts more weakly with water and is significantly attracted to the hydrophobic surfaces of GPAC. CA possess both very high water solubility and intramolecular hydrogen bond and thus is adsorbed by GPAC to a lower extent than 2,4-DCP and 4-CP. Therefore, 2,4-DCP with more hydrophobic group and lower solubility showed more intense adsorption onto GPAC than 4-CP and CA. The comparison of adsorption uptake of phenolic compounds onto different materials is shown in Table 3. This indicates that the GPAC was a promising adsorbent to remove the phenolic compounds.

Table 3 | Comparison of adsorption capacity of activated carbons from other precursors for phenolic compounds

Precursor	Activation method	q_{max} (mmol/g)			References
		CA	4-CP	2,4-DCP	
Coconut spathe	Chemical (KOH)	\	2.139	\	Prashanthakumar *et al.* (2018)
The seed hulls of *Plukenetia africana*	Chemical (CH_3COONa)	\	\	2.334	Garba & Rahim (2016)
Oil palm empty fruit bunch	Chemical ($NH_3{\cdot}H_2O$)	\	\	1.753	Shaarani & Hameed (2011)
Coconut shells	\	1.09	\	\	Suresh *et al.* (2011)
Grapefruit peel	Chemical (H_3PO_4)	1.144	1.677	2.117	This research

Estimation of thermodynamic parameters

To study the thermodynamics of adsorption for CA, 4-CP and 2,4-DCP on GPAC, thermodynamic constants such as enthalpy change ΔH, free energy change ΔG and entropy change ΔS were calculated using equations described in our earlier work (Zou *et al.* 2013a). The values of ΔG, ΔH and ΔS are presented in Table 4.

The negative ΔG values indicated thermodynamically feasible and spontaneous nature of the adsorption. In addition, the negative values of ΔG decreased with the increasing temperature, indicating that adsorption of phenolic compounds onto GPAC becomes more favorable at higher temperatures. The positive value of ΔH showed the endothermic nature for the adsorption process.

It is known that a large proportion of the active sites of the GPAC would be occupied by water molecules via hydrogen bonds. Because the molecular size of phenolic compound is larger than that of water, one phenolic compound molecule adsorbed on active sites would replace more than one surface water molecule. The phenolic compound molecule adsorbed on adsorbents therefore released energy that was not strong enough to overcome the strong hydrogen bonding between the water molecules and adsorbents. The overall adsorption reaction absorbs energy from the surrounding solution, which yields an endothermic reaction (Eren & Afsin 2009). The positive value of ΔS reveals that the randomness of the solid–solution interface increased during the fixation of CA, 4-CP and 2,4-DCP on the active sites of GPAC.

Table 4 | Thermodynamic parameters adsorption of phenolic compounds by GPAC

Phenolic compound	ΔH (kJ/mol)	ΔS (J/(mol· K))	ΔG (kJ/mol)		
			298 K	308 K	318 K
CA	13.21	97	−15.74	−16.58	−17.68
4-CP	7.85	81	−16.19	−16.84	−17.80
2,4-DCP	28.82	157	−18.01	−19.44	−21.15

Regeneration

Regeneration of spent adsorbent and recovery of adsorbate would make the treatment process economical. It may decrease the process cost and the dependency of the process on a continuous adsorbent supply. In this study, the solution of 0.10 mol/L NaOH was studies as a renewable adsorbent. The results illustrated the removal rate of CA, 4-CP and 2,4-DCP reduced after three adsorption–desorption cycles and reached 69.4%, 83.8% and 78.2%, respectively. The percentage of consumption for GPAC was less than 10% after three adsorption–desorption cycles. The complex reactions between phenolic compounds and GPAC may be responsible for the incomplete desorption. Considering the excellent adsorption capacity, small dosage and low cost, the GPAC is still a better choice to remove phenolic compounds in wastewaters.

CONCLUSION

The present study shows that the GPAC prepared from grapefruit peel can be used as an adsorbent for the removal of phenolic compounds from aqueous solutions. The physical properties, surface chemistry and adsorption capacities of activated carbons were comprehensively studied. Adsorption kinetic behavior of CA, 4-CP and 2,4-DCP onto the GPAC was well described by the pseudo-second-order model. The result implies that the adsorption process may be a chemical process. The Freundlich and Koble–Corrigan models were suitable to interpret the adsorption phenomenon of the GPAC and the results implied the adsorption of phenolic compounds on GPAC is heterogeneous. The thermodynamic study indicated that

the adsorption of phenolic compounds was spontaneous and endothermic. After desorption with NaOH of 0.1 mol/L, GPAC could be reused to adsorb phenolic compounds at least three cycles. The result showed that the GPAC could be employed as an alternative to commercial activated carbon for the removal of phenols from wastewater.

ACKNOWLEDGEMENT

This work was supported by the Henan Science and Technology Department in China (No. 162300410016).

REFERENCES

Ahmaruzzaman, M. 2008 Adsorption of phenolic compounds on low-cost adsorbents: a review. *Adv. Colloid Interface Sci.* **143** (1–2), 48.

Ahmaruzzaman, M. & Sharma, D. K. 2005 Adsorption of phenols from wastewater. *J. Colloid Interf. Sci.* **287** (1), 14–24.

Başar, C. A. 2006 Applicability of the various adsorption models of three dyes adsorption onto activated carbon prepared waste apricot. *J. Hazard. Mater.* **135** (1–3), 232–241.

Chai, W. B., Liu, X. Y., Zou, J. C., Zhang, X. Y., Li, B. B. & Yin, T. T. 2015 Pomelo peel modified with acetic anhydride and styrene as new sorbents for removal of oil pollution. *Carbohydr. Polym.* **132**, 245–251.

Chowdhury, S., Mishra, R., Saha, P. & Kushwaha, P. 2011 Adsorption thermodynamics, kinetics and isosteric heat of adsorption of malachite green onto chemically modified rice husk. *Desalination* **265** (1–3), 159–168.

Dabrowski, A., Podkoscielny, P., Hubicki, Z. & Barczak, M. 2005 Adsorption of phenolic compounds by activated carbon–a critical review. *Chemosphere* **58**, 1049–1070.

Dudziak, M. & Werle, S. 2016 Studies on the adsorption of phenol on dried sewage sludge and solid gasification by-products. *Desalin. Water Treat.* **57** (3), 1067–1074.

Dursun, G., Çiçek, H. & Dursun, A. Y. 2005 Adsorption of phenol from aqueous solution by using carbonised beet pulp. *J. Hazard. Mater.* **125** (1–3), 175.

Eren, E. & Afsin, B. 2009 Removal of basic dye using raw and acid activated bentonite samples. *J. Hazard. Mater.* **166** (2–3), 830.

Garba, Z. N. & Rahim, A. A. 2016 Evaluation of optimal activated carbon from an agricultural waste for the removal of para-chlorophenol and 2,4-dichlorophenol. *Process Saf. Environ.* **102**, 54–63.

Gautam, P. K., Gautam, R. K., Banerjee, S., Lofrano, G., Sanroman, M. A., Chattopadhyaya, M. C. & Pandey, J. D. 2015 Preparation of activated carbon from Alligator weed (Alternenthera philoxeroids) and its application for tartrazine removal: isotherm, kinetics and spectroscopic analysis. *J. Environ. Chem. Eng.* **3** (4), 2560–2568.

Huang, H. Y., Luo, L. D., Zhang, H., Lu, Y. Q. & Zhang, D. 2014 Adsorption of Congo red from aqueous solutions by the activated carbons prepared from grapefruit peel. *Applied Mech. Mater.* **529**, 3–7.

Kong, J. J., Yue, Q. Y., Huang, L. H., Gao, Y., Sun, Y. Y., Gao, B. Y., Li, Q. & Wang, Y. 2013 Preparation, characterization and evaluation of adsorptive properties of leather waste based activated carbon via physical and chemical activation. *Chem. Eng. J.* **221** (2), 62–71.

Kumar, A., Kumar, S., Kumar, S. & Kumar, D. V. 2007 Adsorption of phenol and 4-nitrophenol on granular activated carbon in basal salt medium: equilibrium and kinetics. *J. Hazard. Mater.* **147**, 155–166.

Kyzas, G. Z. & Deliyanni, E. A. 2014 Modified activated carbons from potato peels as green environmental-friendly adsorbents for the treatment of pharmaceutical effluents. *Chem. Eng. Res. Des.* **97** (93), 135–144.

Li, A. M., Zhang, Q. X., Chen, J. L., Fei, Z. H., Chao, L. & Li, W. X. 2001 Adsorption of phenolic compounds on amberlite XAD-4 and its acetylated derivative MX-4. *React. Funct. Polym.* **49** (3), 225–233.

Lin, S. H. & Rueyshin, J. 2009 Adsorption of phenol and its derivatives from water using synthetic resins and low-cost natural adsorbents: a review. *J. Environ. Manage.* **90** (3), 1336–1349.

Loredocancino, M., Sotoregalado, E., Garcíareyes, R. B., Cerinocórdova, F. D. J., Garzagonzález, M. T., Alcalárodríguez, M. M. & Dávila-Guzmán, N. E. 2016 Adsorption and desorption of phenol onto barley husk-activated carbon in an airlift reactor. *Desalin. Water Treat.* **57** (2), 845–860.

Mallampati, R., Li, X., Valiyaveettil, S. & Adin, A. 2015 Fruit peels as efficient renewable adsorbents for removal of dissolved heavy metals and dyes from water. *ACS Sustain. Chem. Eng.* **3** (6), 150408093949002.

Marzbali, M. H., Esmaieli, M., Abolghasemi, H. & Marzbali, M. H. 2016 Tetracycline adsorption by H_3PO_4-activated carbon produced from apricot nut shells: a batch study. *Process Saf. Environ.* **102**, 700–709.

Moreno-Castilla, C., López-Ramón, M. V. & Carrasco-MaríN, F. 2000 Changes in surface chemistry of activated carbons by wet oxidation. *Carbon* **38** (14), 1995–2001.

Nowicki, P., Kazmierczak-Razna, J., Pietrzak, R., Nowicki, P., Kazmierczak-Razna, J. & Pietrzak, R. 2016 Physicochemical and adsorption properties of carbonaceous sorbents prepared by activation of tropical fruit skins with potassium carbonate. *Mater. Design* **90**, 579–585.

Pei, Y. Y. & Liu, J. Y. 2012 Adsorption of Pb^{2+} in wastewater using adsorbent derived from grapefruit peel. *Adv. Mater. Res.* **391–392**, 968–972.

Prashanthakumar, T. K. M., Ashok Kumar, S. K. & Sahoo, S. K. 2018 A quick removal of toxic phenolic compounds using porous carbon prepared from renewable biomass coconut spathe and exploration of new source for porous carbon materials. *J. Environ. Chem. Eng.* **6**, 1434–1442.

Shaarani, F. W. & Hameed, B. H. 2011 Ammonia-modified activated carbon for the adsorption of 2,4-dichlorophenol. *Chem. Eng. J.* **169** (1–3), 180–185.

Singh, R. K., Kumar, S., Kumar, S. & Kumar, A. 2008 Development of parthenium based activated carbon and its

utilization for adsorptive removal of *p*-cresol from wastewater. *J. Hazard. Mater.* **155** (3), 523–535.

Sun, Y. Y., Yue, Q. Y., Gao, B. Y., Huang, L. H., Xu, X. & Li, Q. 2012 Comparative study on characterization and adsorption properties of activated carbons with H_3PO_4 and $H_4P_2O_7$ activation employing *Cyperus alternifolius* as precursor. *Chem. Eng. J.* **181–182**, 790–797.

Suresh, S., Srivastava, V. C. & Mishra, I. M. 2011 Isotherm, thermodynamics, desorption, and disposal study for the adsorption of catechol and resorcinol onto granular activated carbon. *J. Chem. Eng. Data* **56**, 811–818.

Thuan, T. V., Quynh, B. T. P., Nguyen, T. D., Thanh Ho, V. T. & Bach, L. G. 2017 Response surface methodology approach for optimization of Cu^{2+}, $Ni^{2+}$and Pb^{2+} adsorption using KOH-activated carbon from banana peel. *Surf. Interface* **6**, 209–217.

Torab-Mostaedi, M., Asadollahzadeh, M., Hemmati, A. & Khosravi, A. 2013 Biosorption of lanthanum and cerium from aqueous solutions by grapefruit peel: equilibrium, kinetic and thermodynamic studies. *Res. Chem. Intermediat.* **41** (2), 559–573.

Weber, W. J. & Morris, J. C. 1963 Kinetics of adsorption on carbon from solution. *J. Sanit. Eng. ASCE* **89**, 31–59.

Yorgun, S. & Yıldız, D. 2015 Preparation and characterization of activated carbons from paulownia wood by chemical activation with H_3PO_4. *J. Taiwan Inst. Chem. Eng.* **53** (1), 122–131.

Yousef, R. I., El-Eswed, B. & Al-Muhtaseb, A. H. 2011 Adsorption characteristics of natural zeolites as solid adsorbents for phenol removal from aqueous solutions: kinetics, mechanism, and thermodynamics studies. *Chem. Eng. J.* **171** (3), 1143–1149.

Zhang, Y., Hu, B. Z. & Huang, Y. M. 2015 Polyethylenimine/grapefruit peel hybrid biosorbent for removal of toxic cdte quantum dots from water. *RSC Advances* **5** (70), 57082–57089.

Zou, W. H., Bai, H. J. & Gao, S. P. 2013a A novel pinus tabulaeformis based adsorbent for the removal of malachite green. *Sep. Sci. Technol.* **48** (18), 2804–2816.

Zou, W. H., Gao, S. P., Zou, X. L. & Bai, H. J. 2013b Adsorption of neutral red and malachite green onto grapefruit peel in single and binary systems. *Water Environ. Res.* **85** (5), 466–477.

Zou, W. H., Zhao, L. & Zhu, L. 2013c Adsorption of uranium(vi) by grapefruit peel in a fixed-bed column: experiments and prediction of breakthrough curves. *J. Radioanal. Nucl. Chem.* **295** (1), 717–727.

First received 11 November 2017; accepted in revised form 29 April 2018. Available online 10 May 2018